

Northumbria Research Link

Citation: McDonald, Tom, Martin, Philip, Patterson, Joseph, Smith, Darren, Giardiello, Marco, Marcello, Marco, See, Violaine, O'Reilly, Rachel, Owen, Andrew and Rannard, Steven (2012) Multicomponent organic nanoparticles for fluorescence studies in biological systems. *Advanced Functional Materials*, 22 (12). pp. 2469-2478. ISSN 1616-301X

Published by: Wiley-Blackwell

URL: <http://dx.doi.org/10.1002/adfm.201103059>
<<http://dx.doi.org/10.1002/adfm.201103059>>

This version was downloaded from Northumbria Research Link:
<https://nrl.northumbria.ac.uk/id/eprint/5861/>

Northumbria University has developed Northumbria Research Link (NRL) to enable users to access the University's research output. Copyright © and moral rights for items on NRL are retained by the individual author(s) and/or other copyright owners. Single copies of full items can be reproduced, displayed or performed, and given to third parties in any format or medium for personal research or study, educational, or not-for-profit purposes without prior permission or charge, provided the authors, title and full bibliographic details are given, as well as a hyperlink and/or URL to the original metadata page. The content must not be changed in any way. Full items must not be sold commercially in any format or medium without formal permission of the copyright holder. The full policy is available online: <http://nrl.northumbria.ac.uk/policies.html>

This document may differ from the final, published version of the research and has been made available online in accordance with publisher policies. To read and/or cite from the published version of the research, please visit the publisher's website (a subscription may be required.)

ABSTRACT

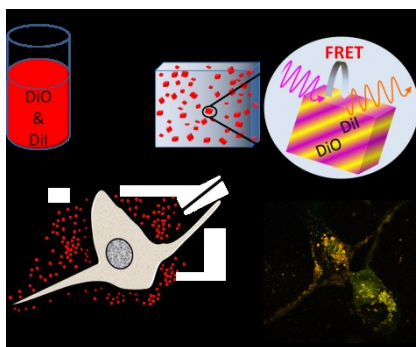
Dual-component organic nanoparticles are prepared by a modified emulsion-templated freeze-drying approach to give an aqueous nanosuspensions showing Fluorescence (Förster) Resonance Energy Transfer (FRET) from within a distribution of single nanoparticles, dissolution of these particles results in loss of this FRET signal. Incubation of the particles with cells and analysis by confocal microscopy allows spatial and physical monitoring of the particles after internalization.

Keywords: Poorly water-soluble, nanoparticles, nanosuspension, cellular uptake, FRET.

By *Tom O. McDonald, Philip Martin, Joseph P. Patterson, Darren Smith, Marco Giardiello, Marco Marcello, Violaine See, Rachel K. O'Reilly, Andrew Owen,* and Steve Rannard.**

Multi-component Organic Nanoparticles for Fluorescence Studies in Biological Systems

ToC figure ((55 mm broad, 50 mm high, or 110 mm broad, 20 mm high))



includinDOI: 10.1002/adma.((please add manuscript number))

Multi-component Organic Nanoparticles for Fluorescence Studies in Biological Systems

By *Tom O. McDonald, Philip Martin, Joseph P. Patterson, Darren Smith, Marco Giardiello,*

Marco Marcello, Violaine See, Rachel K. O'Reilly, Andrew Owen, and Steve Rannard.**

[*] Prof. S. Rannard. Dr. T. O. McDonald. Dr. M. Giardiello.
Department of Chemistry
University of Liverpool
Crown Street
Liverpool, L69 7ZD (United Kingdom)
E-mail: srannard@liv.ac.uk

[*] Prof. A. Owen. Dr. P. Martin. Dr. D. Smith.
Department of Molecular and Clinical Pharmacology
University of Liverpool, Block H
70 Pembroke Place
Liverpool, L69 3GF, (United Kingdom)
E-mail: aowen@liv.ac.uk

Dr. R. K. Reilly. J. P. Patterson.
University of Warwick
Department of Chemistry
Gibbet Hill Road,
Coventry, CV4 7AL, (United Kingdom)

Dr. V. See. Dr. M. Marcello.
Centre for Cell Imaging
Institute of Integrative Biology
University of Liverpool
Liverpool, L69 7ZB, (United Kingdom)

Keywords: Poorly-water soluble, nanoparticles, nanosuspension, cellular uptake, FRET.

The formation of dual-component organic nanoparticles by a modified emulsion-templated freeze-drying approach has led to aqueous nanosuspensions showing Fluorescence (Förster) Resonance Energy Transfer (FRET) from within a distribution of single nanoparticles. The combination of both FRET dyes within dual-component nanoparticles (<200 nm) allows the spatial and physical monitoring of the particles as the FRET signal is lost on dissolution and

breakdown of the nanoparticles. The monitoring of accumulation by Caco-2 cells and macrophages shows very limited internalization within the non-phagocytic cells. Conservation of FRET within the macrophages confirms extensive whole-particle internalization. The cellular permeability through Caco-2 monolayers was also assessed and movement of intact dual-component particles was observed, suggesting a mechanism for enhanced pharmacokinetics *in vivo*.

1. Introduction

The use of nanosuspensions, particles of pure drug in the sub-micron size range,^[1] has been heralded as an approach to address the issue of formulating poorly soluble active pharmaceutical ingredients (API)^[2-9] and has been successful in producing a range of new medicines, dosed daily in clinics globally. These include the immunosuppressant Rapamune® (rapamycin), the chemotherapy-induced nausea prevention medicine Emend® (aprepitant) and the hypercholesterolemia treatment TriCor® (fenofibrate). The solid drug particles do not utilize a drug carrier or a drug vehicle, such as vesicles, micelles or pegylation,^[10] to overcome poor solubility, therefore each particle conveys high drug content, offering an efficient way to deliver drugs to, and/or into, cells. Additionally, formulating a poorly-soluble drug as a nanosuspension has been shown to enhance dissolution rate and improve bioavailability^[7, 11, 12] over conventional drug formulation approaches.

The *in vivo* behavior of drugs in various nanoparticle forms has been subject to a considerable amount of research.^[13-15] Ongoing study continues to investigate the cellular uptake and accumulation of a wide range of nanoparticles, nanoparticulate drug delivery systems and colloidal particles with a specific emphasis on toxicity.^[14, 16] Nanosuspensions, typically composed of aggregates or crystals of poorly-soluble organic molecules, have a finite solubility and do not utilize a nanoscopic vehicle for delivery, therefore the nanoparticles will undergo continuous dissolution within the body.

The Caco-2 cell line, originating from human colorectal carcinoma, has been shown to spontaneously differentiate in culture to form a confluent monolayer with morphological and functional similarities to the small intestinal epithelium.^[17] As a result of these characteristics the Caco-2 monolayer has been developed as a model to study a range of therapeutic agents and delivery vehicles (microparticles,^[18] nanoparticles^[19] and nanocomplexes^[20]). Hu and co-workers compared the uptake into Caco-2 cells (human intestinal, non-phagocytic) and phagocytic cells (mouse macrophage RAW cells) of charcoal nanoparticles and a pyrene nanosuspension, using optical microscopy.^[21] Both types of particle displayed similar uptake behavior; limited in the Caco-2 cells but extensive in the RAW cells. The limitations of optical microscopy led to a lack of clarity regarding whether the pyrene particles were indeed internalized intact or transported as dissolved molecules with subsequent accumulation within the cell. Other studies have shown that nanosuspensions of hydrophobic drugs, produced by milling, gave an increase in the apparent permeability through a Caco-2 monolayer compared to un-milled drug. The authors suggested that improvement of oral bioavailability was due to increased dissolution rather than movement of particles through the cells of the gastrointestinal (GI) tract.^[2] The transport and fate of nanosuspensions within the body is therefore relatively poorly understood with respect to; a) whether particles, when orally dosed, cross the GI tract and enter the circulation intact, b) whether dissolution occurs before cellular uptake and c) whether particles remain intact over considerable timescales after uptake into phagocytic cells. Accurate monitoring of the physical state of nanosuspensions, and their dissolution, is therefore key to the study of cellular uptake.

Cellular uptake of block copolymer micelle drug delivery vehicles was investigated by Cheng and co-workers^[22] using Fluorescence (Förster) Resonance Energy Transfer (FRET).^[23] FRET relies upon non-radiative energy transfer (long-range, <10 nm, dipole-dipole coupling) from a donor fluorophore in an electronic excited state, to a second

fluorophore, the acceptor. A FRET signal is observed when the donor molecule is excited and transfers its energy to the acceptor, resulting in acceptor emission.

The micelles were loaded with a pair of FRET dyes (donor and acceptor) and were considered intact if a FRET signal was observed, indicating close proximity of the donor and acceptor fluorophores within the hydrophobic interior of the micelle. Decomposition of the micelles, or release of dye from the micelle, caused a loss in the FRET signal as the two fluorophore molecules became dissociated resulting in loss of energy transfer. We were interested in using the same concept to monitor the physical state of the particles during cellular uptake however, traditional top-down approaches used to produce nanosuspensions (such as milling or high-pressure homogenization) are not suitable for producing nanoparticles that contain two different organic molecules.

In this paper we use a simple modified emulsion-templated freeze-drying method^[24] to produce a dual-component hydrophobic nanosuspension where particles contain a FRET fluorophore pair. We demonstrate that these particles indeed contain both fluorophores and that dissolution of the particles was accompanied by dramatic reduction in the FRET signal. These particles were used to investigate cellular uptake into human monocyte derived macrophages (activated THP-1 cells - A-THP-1) and Caco-2 cells before assessing the permeability of these particles through a Caco-2 cell monolayer.

2. Results and Discussion

2.1. Nanosuspension synthesis and characterization.

Single component, containing one fluorophore, and dual-component, containing both acceptor and donor fluorophores, nanosuspensions were prepared by a modified emulsion-templated freeze-drying method (**Fig. 1**). Briefly, 3,3'-dioctadecyloxycarbocyanine perchlorate (DiO) and 1,1'-dioctadecyl-3,3',3',3'-tetramethylindocarbocyanine perchlorate

(DiI) were dissolved in chloroform either individually or together in various ratios. The chloroform solutions were emulsified with an aqueous solution containing a non-ionic polyethylene oxide hexadecyl ether surfactant (Brij 58) and 80% hydrolyzed polyvinyl alcohol (PVA). After immediate freezing of the emulsions in liquid nitrogen the samples were lyophilized, removing the water and chloroform to yield a porous solid. Addition of water to the products resulted in dissolution of the water-soluble polymer/surfactant matrix and release of the hydrophobic fluorophores as stabilized nanosuspensions.

Analysis of the single component and dual-component dispersions by dynamic light scattering (DLS) showed mono-modal distributions with similar mean sizes (**Fig. 2A**). The z-averages of the nanosuspensions were 184 nm, 123 nm and 165 nm (+/- 9 nm) with polydispersity indexes (defined in ISO13321) of 0.265, 0.255 and 0.228 (+/- 0.07) for single-component DiO, single-component DiI and DiO₅₀/DiI₅₀ dual-component particles, respectively. Additionally, the nanosuspensions were stable for at least 1 month with average size and distribution remaining unchanged (supporting information (SI) Figure 1S). Zeta potential measurements of the nanosuspensions also indicated similar values which appeared to be largely independent of composition (10-12 mV (+/- 4 mV)), the minor cationic charge of the nanosuspensions arising from DiO and DiI. The low zeta potentials suggest that colloidal stability was given by the steric stabilization from adsorbed PVA and the overall similarity of the particles was considered appropriate for direct comparative studies. The nanoparticles were imaged using a graphene oxide (GO) support. Previous reports have demonstrated the advantages of using GO as a low contrast support for transmission electron microscopy (TEM)^[25-28] and recently as a support for multi-technique imaging by TEM, scanning electron microscopy (SEM) and atomic force microscopy (AFM).^[29] The three techniques can be performed concurrently on the same GO-grid, simplifying the collection of complementary images. Furthermore the nature of the GO grid allows for images to be collected unstained

and uncoated, minimizing misinterpretation of data and allowing for more accurate correlation of results. The morphology of the particles was first examined by TEM and SEM (**Fig. 2B&C**) and irregular, asymmetric shapes with a high aspect ratio were observed using both techniques. Characterization of the particles by AFM (**Fig. 2D&E**) yielded a similar morphology; flattened asymmetric particles in the same size range as determined by SEM and TEM. Although the sizes determined by TEM, SEM and AFM appear to be smaller than the DLS measurements, all values are consistent in showing the formation of <200 nm particles, especially when considering the approximation to spheres that is inherent in DLS measurement. Analysis of the materials by x-ray powder diffraction (XRPD) revealed that the particles were composed of the fluorophores in an amorphous state (SI Figure 2S).

2.2 Characterizing nanosuspension fluorescence and FRET emission. FRET is a well established method used primarily to study protein interactions and conformation changes *in situ*.^[30] FRET occurs when two fluorophores with an overlap in their emission and excitation are within close proximity (less than 10 nm). FRET is observed as a decrease in the donor emission along with a concomitant increase in the emission of the acceptor occurring through the energy transfer from donor to acceptor. An unequivocal FRET signal therefore clearly demonstrates the presence of dual-component nanoparticles, i.e. single particles containing both fluorophores.

DiO and DiI are a well reported FRET fluorophore pair and excitation of DiO at relatively low wavelengths will result in emission from DiI if the dyes are located within close proximity (**Fig. 3E**). In order to verify the occurrence of FRET, and therefore the co-localisation of the two fluorophores within single combination particles, fluorescence spectra of both single and dual-component nanoparticles were obtained (**Fig. 3**). An excitation wavelength ($\lambda_{\text{ex}}^{\text{DiO}}$) of 420 nm was found to give good discrimination between DiO and DiI single-component nanosuspensions (SI Figure 5S); we found no effect on the emission peak wavelength when varying the excitation wavelength of any of the fluorescent

nanosuspensions, therefore no red-edge excitation shift ^[31, 32] was observed. The single-component nanosuspension of DiO showed a peak emission (λ_{em}^{DiO}) at 545 nm (**Fig. 3A**), while the single-component nanosuspension of DiI displayed a weak emission (λ_{em}^{DiI}) at 598 nm (**Fig. 3B**) due to poor excitation efficiency at 420 nm. Dual-component DiO₅₀/DiI₅₀ nanosuspensions exhibited a single strong emission λ_{em}^{DiI} peak (598 nm) when excited at 420 nm (**Fig. 3C**) and no emission at 545 nm. The absence of a λ_{em}^{DiO} peak and the presence of a sole λ_{em}^{DiI} peak when exciting the nanosuspension at λ_{ex}^{DiO} corresponds to efficient energy transfer between the two fluorophores. The extent to which FRET occurs may be quantified using the FRET ratio $I_{DiI}/(I_{DiO} + I_{DiI})$, where I_{DiO} and I_{DiI} are the fluorescence intensities at 545 and 598 nm respectively when exciting the nanosuspensions at λ_{ex}^{DiO} (420 nm). The DiO₅₀/DiI₅₀ dual-component nanosuspension displayed a FRET ratio of 0.98; almost complete energy transfer.

The potential for the FRET behavior originating from the close proximity of separate particles of each fluorophore was studied by measuring the fluorescence of a 1:1 mixture of single component nanosuspensions of DiO and DiI (**Fig. 3D**). Two distinct emission peaks at 540 and 598 nm were observed when the mixture was excited at 420 nm (FRET ratio of 0.30) indicating a low level of energy transfer occurring between the fluorophores when in separate particles and supporting the presence of DiO and DiI within the dual-component nanoparticles.

The relative ratio of the donor to acceptor fluorophore within the dual-component particles was readily varied using the emulsion-templated freeze-drying nanoparticle synthesis. Dual-component particles ranging in mean diameters between 120 – 255 nm were produced over a range of compositions from 100% DiO to 100% DiI. As the relative amount of DiO in the dual-component particles was increased, the average particle diameter in the dispersions was found also to generally increase (SI Figure 3S) at a constant PVA/Brij 58/total fluorophore ratio (weight %). Analysis of the fluorescence emission (**Fig. 4A**) of dual-component

nanosuspensions with varying DiO/DiI ratios showed that very low additions of acceptor (e.g. DiO₉₀/DiI₁₀) yielded a large increase in acceptor emission and subsequent decrease in donor emission (with a FRET ratio of 0.87). Further increases in the DiI content resulted in decreasing acceptor emission possibly due to increased self-quenching within the solid nanoparticles. Increasing the DiI content to DiO₇₀/DiI₃₀ yielded spectra with complete absence of the donor emission when the nanosuspensions were excited at $\lambda_{\text{ex}}^{\text{DiO}}$; thus all energy is transferred to the acceptor, DiI (a FRET ratio of 0.97). As a FRET ratio is defined as the acceptor emission divided by the sum of acceptor and donor emission, we have calculated FRET ratios across all compositions, understanding that a FRET ratio of a single-component nanosuspension of DiI will have a value very close to 1, similarly a single-component DiO nanosuspension has a value very close to zero. These values are clearly not derived from FRET however this approach allows comparison across the full composition range available. Varying the ratio of individual DiO particles to DiI particles in a mixture of the single-component nanosuspensions led to completely different behavior (**Fig 4B**). Acceptor emission was not found to increase at any ratio of DiO/DiI, probably due to the isolation of donor and acceptor within individual particles. The potential for FRET is therefore restricted to either a) surface contact of the nanoparticles or b) energy transfer between the low concentrations of dissolved molecules of DiO and DiI (either in solution or within surfactant/polymer assemblies). The observed increase in FRET ratio (with increasing DiI content) is purely related to the subsequent reduction in DiO at increased DiI levels (to maintain constant total fluorophore concentration) and resulting decreased DiO emission.

Particle breakdown or dissolution may also be observed by monitoring the FRET signal within the dual-component nanoparticles. As the particles begin to dissolve the two fluorophores are no longer co-localized within the particles and the distance between the donor and acceptor increases. For example, after dissolution of the DiO₅₀/DiI₅₀ dual-component nanosuspension in methanol, FRET was found to be greatly reduced (**Fig. 4C**)

with the FRET ratio (the wavelengths chosen to represent the two fluorophores are adjusted to account for blue shift) reduced from 0.98 in water to 0.19 as a dissolved solution. Additionally, DLS analysis of the methanol solutions did not yield sufficient scattering for accurate size measurement, providing further evidence that particle dissolution had occurred. When a similar methanol dissolution was performed on a mixture (1:1) of DiO and DiI single-component dispersions, nearly identical fluorescence spectra were observed, supporting our conclusions that the observed FRET signal from the single nanoparticle mixtures arises from low level energy transfer at the molecular or particle surface level. Blue shifting of the emission was observed for both DiO (-39 nm) and DiI (-28 nm) along with an increase in emission intensity upon dissolution. This finding was likely due to separation of fluorophores within the excimer assemblies present within the nanoparticles and a subsequent loss of self-quenching.^[33] The dramatic reduction in FRET and FRET ratio during dual-component nanoparticle dissolution provides a useful measure allowing monitoring of the physical state of the nanosuspensions.

In order to verify that the dual-component nanosuspensions can be used at the appropriate concentrations for cellular uptake studies, serial dilution experiments were carried out using the DiO₅₀/DiI₅₀ dual-component nanosuspension to determine whether, at such low concentrations, nanoparticle dissolution would occur. (**Fig. 4D**). The FRET signal (acceptor emission from excitation at $\lambda^{\text{DiO}}_{\text{ex}}$) decreased in a linear manner as the nanosuspensions were diluted. The apparent decrease in the FRET ratio at very high dilutions was due to the very low acceptor emission relative to the noise in the measurement of the donor emission. The data suggest limited dual-component nanosuspension dissolution in the low concentration range required for cellular uptake and transport measurements using fluorescence spectroscopy. The dual-component nanoparticles are therefore useful probes for cellular uptake/transport experiments, allowing the combined spatial reporting and indication of physical state of the nanoparticles within the experiment.

However, the 1:1 mixture of DiO and DiI single-component nanoparticles displayed a clear donor emission (λ_{em}^{DiO}) at 537 nm, slightly blue-shifted from the bulk measurements (Fig. 3A) of 545 nm potential evidence of some dissolution of the DiO single-component nanoparticles. Interestingly, the mixture of DiO and DiI single-component nanoparticles also showed reduced donor emission inside the cell compared to the initial mixture of nanosuspensions (SI Figure 11S B). This indicates that the single-component donor and acceptor nanoparticles had been individually internalised and appear to accumulate within close proximity in the same regions of the cell. The FRET ratio (after 24 hours) was found to be significantly (with a p-value of 0.046) higher for the dual-component particles (0.89; **Fig. 6D**) than for the mixture of single-component particles (0.74; **Fig. 6E**). pH studies of the dual-component nanosuspensions in the absence of cells (SI Figure 12S), showed identical fluorescence spectra over a range of pH values (4.8-8.9). Investigation of the FRET ratios over the three time points showed that the FRET ratios remained constant over time for both dual-component (**Fig. 6F**) and the mixture of single-component nanoparticles (**Fig. 6G**), while the single-component particles seemed to display slightly greater accumulation. Comparison of the FRET ratios from within the cell (after 24 hours) against those of the aqueous dispersion (SI Figure 11S C) showed that the dual-component nanoparticles may have undergone slight particle dissolution as the FRET ratio decreased from 0.97 to 0.89. Overall, these findings provide strong evidence that the dual-component nanoparticles are internalized into A-THP-1 cells as intact structures with only minor dissolution.

Transport of organic nanoparticles through Caco-2 cell monolayers was studied. This model has tight junctions and a luminal (apical) and systemic compartment (basolateral) mimicking the gut and blood, respectively.^[38] DiO₅₀/DiI₅₀ dual-component nanosuspensions were compared to a 1:1 mixture of DiO and DiI single-component nanosuspensions by addition to the apical compartment at a concentration relevant to *in vivo* drug particles dosed orally (50 μ M). After 18 hours the basolateral chamber (systemic circulation mimic) was sampled and

analyzed by fluorimetry (**Fig. 7**) to quantify the concentration of fluorophore that had transported through the monolayer. The low concentrations of fluorophore detected in the basolateral chamber indicated a low level of transport and required an excitation wavelength of 458 nm to increase overall emission from the samples. This wavelength provides less discrimination between FRET and DiI excitation/emission but this compromise was necessary to increase sensitivity and allow accurate fluorophore quantification.

The emission spectra (**Fig. 7A**) of the basolateral compartment after 18 hours showed an observable fluorescence when applying either the dual-component or mixture of single-component nanosuspensions to the apical compartment. Two specific peaks were observed in the spectra, one at approximately 505 nm, corresponding to DiO emission, and a second peak at approximately 575 nm assigned to DiI emission. In both cases, the dual-component and mixture of single-component nanosuspensions displayed blue shifted spectra (similar λ_{\max} values as those observed in methanol) suggesting the presence of a majority of dissolved molecules after permeation. The emission spectra from the basolateral samples when using dual-component nanosuspensions displayed a noticeably stronger emission for both DiO and DiI (FRET ratio = 0.61) than samples taken when using a mixture of single-component nanosuspensions (FRET ratio = 0.52). The observed FRET ratio however provides no accurate quantification of the levels of fluorophore that has transported. To understand the physical nature of the nanosuspensions during transport it is important to quantify the acceptor fluorophore individually by using a second excitation wavelength of 550 nm (**Fig. 7B**). The wavelength and emission intensity of DiI was approximately equal for both the dual-component and the single-component nanosuspensions, implying that the same amount of DiI fluorophore had passed through the cell monolayer into the receiver well. The differences in FRET ratio (excitation at 458 nm) are therefore derived from the proximity of DiO and DiI in the basolateral chamber which suggests that at least some of the dual-component nanoparticles crossed the cell monolayer as intact particles; DiO and DiI permeating together

in a single nanoparticle. The observation of a FRET signal in the basolateral compartment, (Fig 7A) coupled with the low level of intracellular FRET signal in Caco-2 cells from our accumulation studies, (SI Figure 8S) would also indicate that the nanoparticles may have traversed the monolayer *via* a paracellular route, between the cells, rather than by permeation through the cell. Paracellular movement of nanoparticles has been shown previously,^[39] in the presence of chitosan either as particles or as dissolved molecules, enhancing drug transition through Caco-2 monolayers.^[40-42] It has been suggested that chitosan, carrying a permanent positive charge, causes reversible opening in the paracellular channels due to electrostatic interactions resulting in disruption of the tight junctions.^[42, 43] It is possible that the cationic character of our dual-component nanoparticles led to a similar disruption within the tight junctions. The potential for paracellular movement of the nanoparticles presented here is not completely intuitive, as our particles contain no chitosan. Further study, which may add considerable understanding to the enhanced bioavailability and pharmacokinetics observed for many nanosuspension medicines, is therefore required.

3. Conclusions

Unlike previous nanosuspension techniques, we have controllably generated a range of single-component and dual-component fluorescent nanoparticles (< 200nm) with varying composition using an emulsion-templated freeze-drying method. By selecting a FRET-pair of fluorophores, we were able to determine the different fluorescence properties of mixtures of single component nanosuspensions and dual-component nanoparticles. The highly efficient FRET observed within the dual-component nanosuspensions allows the reporting of nanoparticle physical state using conventional fluorescence microscopy. The application of the dual-component nanosuspensions to cellular uptake studies have demonstrated particle localization within, or at the surface, of the cells studied and the presence of intact particles within macrophages after only 4 hours incubation. Limited internalization of nanoparticles

was seen within Caco-2 cells but permeation experiments suggested the potential for paracellular transport of nanoparticles across an epithelial monolayer with tight junctions. The passage of intact nanoparticles across intestinal epithelial cells has implications that require further study as this may clarify mechanisms of modified *in vivo* behavior of current and potential nanoparticle therapies.

3. Experimental

Materials. Unless stated otherwise, all of the reagents and solvents were used as received. 3,3'-dioctadecyloxacarbocyanine perchlorate (DiO) and 1,1'-dioctadecyl-3,3,3',3'-tetramethylindocarbocyanine perchlorate (DiI) were purchased from Invitrogen. Poly(vinyl alcohol) (PVA; 80 % hydrolyzed, MW 9,000-10,000), Brij 58, RPMI-1640, phorbol 12-myristate 13 acetate (PMA) and Dulbecco's modified eagle's medium were purchased from Sigma-Aldrich.

Particle synthesis. Particles were prepared by emulsion templating followed by freezing and lyophilization. DiO or DiI were dissolved in chloroform at 10 mg/ml. 100 μ l of DiO or DiI solution (or 50 μ l of DiO and 50 μ l DiI for the dual-component particles) was added to a 3 ml vial. To this organic solution 133 μ l of Brij 58 (22.5 mg/ml in DI water) and 267 μ l of PVA (80% hydrolyzed) (22.5 mg/ml in DI water) were added. An emulsion was formed by sonicating the sample for 12 seconds using a Covaris S2x with a duty cycle of 20, an intensity of 10 and 500 cycles/burst in frequency sweeping mode. The samples were then immediately frozen in liquid nitrogen. Lyophilizing for three days (Virtis benchtop K) yielded a porous solid that upon addition of water produced a nanosuspension.

Particle characterization. The average size and zeta potential of the nanosuspensions were measured at 1 mg/ml at a temperature of 25°C using a Malvern Zetasizer Nano ZS equipped with a 4mW He-Ne, 633nm laser. The z-average diameters and polydispersity indexes were obtained by DLS. Malvern Zetasizer software version 6.20 was used for data analysis. Zeta

potential measurements were also carried out at 1 mg/ml, at 25°C, a pH of 6.5, using disposable capillary zeta cells. The fluorescence spectra of the nanoparticle dispersion were obtained on a PerkinElmer LS55 using disposable UV-grade PMMA cuvettes with a path length of 1 cm. For fluorescence spectrometry the emulsion-templated solids were dispersed in deionised water to a fluorophore concentration of 0.032 mg/ml. For the dissolution in methanol experiments the solids were first dispersed in water at 1 mg/ml which was then dissolved in methanol to a concentration of 0.016 mg/ml. The excitation and emission slits were unchanged when measuring spectra that were directly compared and no normalization of the data was carried out.

Electron microscopy. Prior to electron microscopy the dual-component sample (DiO₅₀/DiI₅₀) was dialyzed for 4 days using a biodialyzer fitted with cellulose acetate membranes with a molecular weight cut-off of 50,000 daltons (Harvard Apparatus) (dialysis was found to have no effect on particle size (SI Figure 4S)). All electron microscopy images were obtained with the sample deposited on a modified TEM grid, these were prepared as follows: Solutions of graphene oxide^[28] were synthesized as previously reported. GO solutions (0.10 - 0.15 mg/ml) were sonicated for 30 seconds prior to use. Lacey carbon grids (400 Mesh, Cu) (Agar Scientific) were cleaned using air plasma from a glow-discharge system (2 min, 20 mA). One drop (~ 0.08 ml) of the sonicated GO solution was deposited onto each grid and left to air-dry for ~ 30 min. 4 µL of sample (at 0.5 mg/ml) was pipetted onto a GO grid and blotted immediately blotted away using a piece of filter paper. TEM images were recorded on either a JEOL 2000FX TEM or a JEOL 2100 equipped with Gatan Orius digital camera, both were operated at 200kV. While, a Zeiss Supra55VP was used to acquire the SEM images, operated at an accelerating voltage of 20 kV.

Atomic force microscopy (AFM). AFM images were taken in tapping mode on a Multimode AFM with Nanoscope IIIA controller with Quadrex. Silicon AFM tips were used with nominal spring constant and resonance frequency of 3.5 Nm⁻¹ and 75 kHz (MikroMasch

emission. For the spectral analysis the emission between 500-700 nm was collected at 10 nm intervals. Data was captured using Zeiss Zen software (Zeiss, Jena, Germany) and analyzed using Zeiss LSM image browser (version 4,2,0,121).

Transwell experiment. Caco-2 cells were inoculated (4×10^4 cells per well) onto Corning 24 Well HTS Transwell support plates (Corning Ltd) and allowed to propagate, differentiate and polarize over a 21 day period as previously described,^[38] where the cell media (DMEM containing 15% FBS) was replaced every other day. The emulsion-templated solids were dispersed in deionised water to a fluorophore concentration of 1.0 mg/ml. These nanosuspensions were then diluted to 50 μ M in Hanks buffer containing 0.5mM L-glutamine. These nanosuspensions were added to the apical compartment (intestinal lumen mimic) and transcellular permeability was assessed by fluorimetry (PerkinElmer LS55) after pooling the recipient buffer contained in 5 basolateral compartments after 18 hours incubation.

Acknowledgements

The authors wish to thank the RCUK for Grand Challenge Grant Funding (EP/G066272/1) that funded the research. Dr Dave Adams is thanked for access to his fluorimeter. The supporting information contains the following additional results: DLS analysis of the size stability of the dual-component nanosuspension; PXRD of the freeze-dried monoliths containing fluorescent nanoparticles; DLS analysis of the effect of varying the composition of the dual-component nanosuspensions; DLS analysis of the effect of dialysis on the dual-component nanosuspension; absorption and excitation spectra for single and dual-component nanosuspensions; effect of cell media on dual-component particle size; orthogonal sections and confocal microscopy sections of the A-THP-1 and Caco-2 cells dosed with dual-component particles; confocal microscopy images showing the selected ROIs used for spectral analysis; brightfield images corresponding to the images obtained by confocal fluorescence microscopy; comparison of fluorescence emission of dual-component and a

- [21] Y. Lai, P.-C. Chiang, J. D. Blom, N. Li, K. Shevlin, T. G. Brayman, Y. Hu, J. G. Selbo, L. G. Hu, *Nanoscale Research Letters* **2008**, *3*, 321.
- [22] H. T. Chen, S. W. Kim, L. Li, S. Y. Wang, K. Park, J. X. Cheng, *Proceedings of the National Academy of Sciences of the United States of America* **2008**, *105*, 6596.
- [23] E. A. Jares-Erijman, T. M. Jovin, *Nat Biotech* **2003**, *21*, 1387.
- [24] H. Zhang, D. Wang, R. Butler, N. L. Campbell, J. Long, B. Tan, D. J. Duncalf, A. J. Foster, A. Hopkinson, D. Taylor, D. Angus, A. I. Cooper, S. P. Rannard, *Nat Nano* **2008**, *3*, 506.
- [25] N. R. Wilson, P. A. Pandey, R. Beanland, J. P. Rourke, U. Lupo, G. Rowlands, R. A. Romer, *New Journal of Physics* **2010**, *12*, 125010.
- [26] J. Sloan, Z. Liu, K. Suenaga, N. R. Wilson, P. A. Pandey, L. M. Perkins, J. P. Rourke, I. J. Shannon, *Nano Letters* **2010**, *10*, 4600.
- [27] R. S. Pantelic, J. C. Meyer, U. Kaiser, W. Baumeister, J. M. Plitzko, *Journal of Structural Biology* **2010**, *170*, 152.
- [28] N. R. Wilson, P. A. Pandey, R. Beanland, R. J. Young, I. A. Kinloch, L. Gong, Z. Liu, K. Suenaga, J. P. Rourke, S. J. York, J. Sloan, *ACS Nano* **2009**, *3*, 2547.
- [29] J. P. Patterson, A. M. Sanchez, N. Petzetakis, T. P. Smart, I. I. I. T. H. Epps, I. Portman, N. R. Wilson, R. K. O'Reilly, *Soft Matter* **2012**. DOI: 10.1039/C2SM07040E.
- [30] B. N. G. Giepmans, S. R. Adams, M. H. Ellisman, R. Y. Tsien, *Science* **2006**, *312*, 217.
- [31] A. Chattopadhyay, *Chemistry and Physics of Lipids* **2003**, *122*, 3.
- [32] A. P. Demchenko, *Luminescence* **2002**, *17*, 19.
- [33] D.-B. Kim, C.-H. Choi, S.-H. Lee, Y.-S. Lee, K. Zong, S.-C. Yu, *Colloids and Surfaces A: Physicochemical and Engineering Aspects* **2007**, *303*, 201.
- [34] M. P. Desai, V. Labhasetwar, E. Walter, R. J. Levy, G. L. Amidon, *Pharmaceutical Research* **1997**, *14*, 1568.
- [35] I. Behrens, A. I. V. Pena, M. J. Alonso, T. Kissel, *Pharmaceutical Research* **2002**, *19*, 1185.
- [36] E. Roger, F. Lagarce, E. Garcion, J. P. Benoit, *Journal of Controlled Release* **2009**, *140*, 174.
- [37] S. Mitragotri, J. Lahann, *Nat Mater* **2009**, *8*, 15.
- [38] I. Hubatsch, E. G. E. Ragnarsson, P. Artursson, *Nat. Protocols* **2007**, *2*, 2111.
- [39] Y.-H. Lin, C.-K. Chung, C.-T. Chen, H.-F. Liang, S.-C. Chen, H.-W. Sung, *Biomacromolecules* **2005**, *6*, 1104.
- [40] A. M. M. Sadeghi, F. A. Dorkoosh, M. R. Avadi, M. Weinhold, A. Bayat, F. Delie, R. Gurny, B. Larijani, M. Rafiee-Tehrani, H. E. Junginger, *European Journal of Pharmaceutics and Biopharmaceutics* **2008**, *70*, 270.
- [41] D. Vllasaliu, R. Exposito-Harris, A. Heras, L. Casettari, M. Garnett, L. Illum, S. Stolnik, *International Journal of Pharmaceutics* **2010**, *400*, 183.
- [42] A. Sadighi, S. N. Ostad, S. M. Rezayat, M. Foroutan, M. A. Faramarzi, F. A. Dorkoosh, *International Journal of Pharmaceutics* **2012**, *422*, 479.
- [43] T.-H. Yeh, L.-W. Hsu, M. T. Tseng, P.-L. Lee, K. Sonjae, Y.-C. Ho, H.-W. Sung, *Biomaterials* **2011**, *32*, 6164.

FIGURE 3

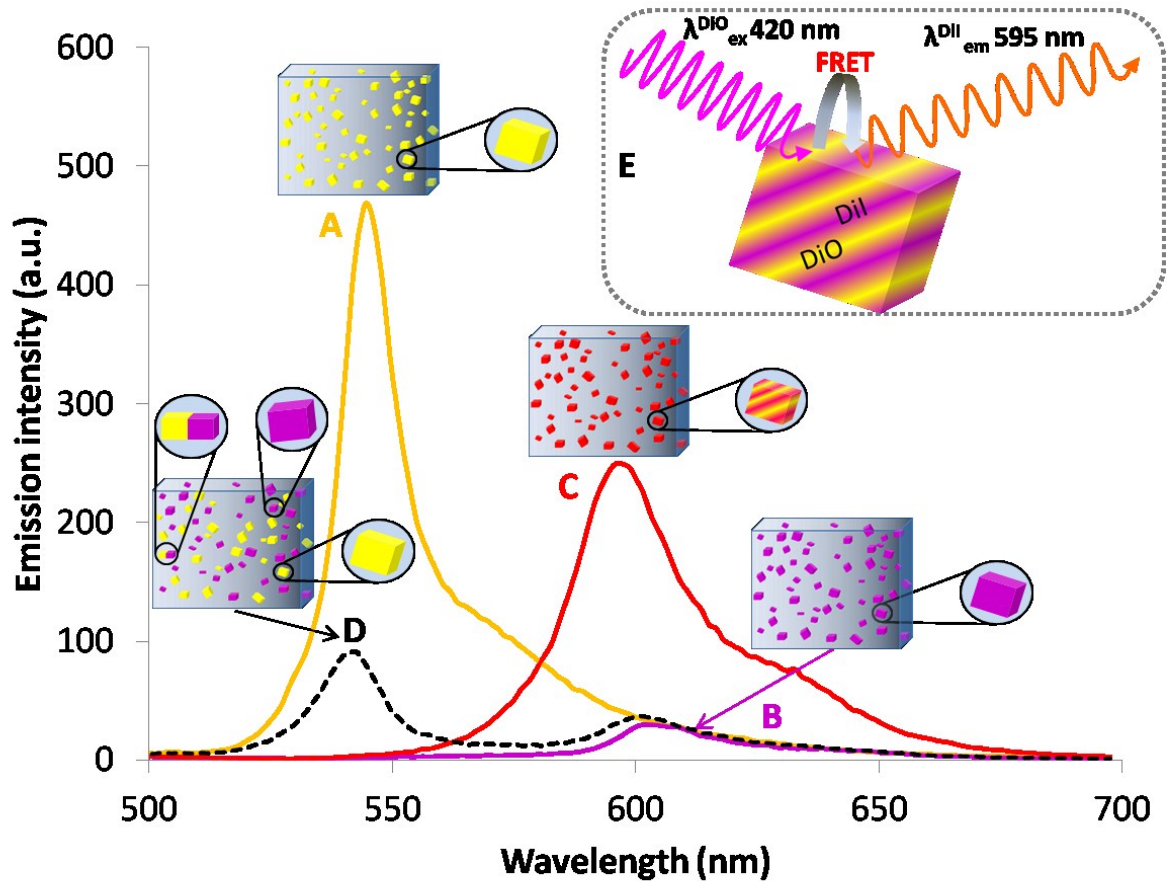


FIGURE 3 CAPTION

Figure 3. Fluorescence emission spectra of different nanosuspensions obtained upon excitation at 420 nm (at an overall nanoparticle concentration of 0.032 mg/ml). A) DiO single-component nanosuspension (yellow); B) DiI single-component nanosuspension (purple); C) DiO₅₀/DiI₅₀ dual-component nanosuspension (red; FRET ratio = 0.98); D) 1:1 mixture of both single-component DiO and single-component DiI nanosuspensions (0.016 mg/ml of DiO nanosuspension and 0.016 mg/ml of DiI nanosuspension (total fluorophore concentration 0.032 mg/ml)) (Black dotted line; FRET ratio 0.30); E) A scheme for the FRET signal from the dual-component nanoparticles.

FIGURE 6

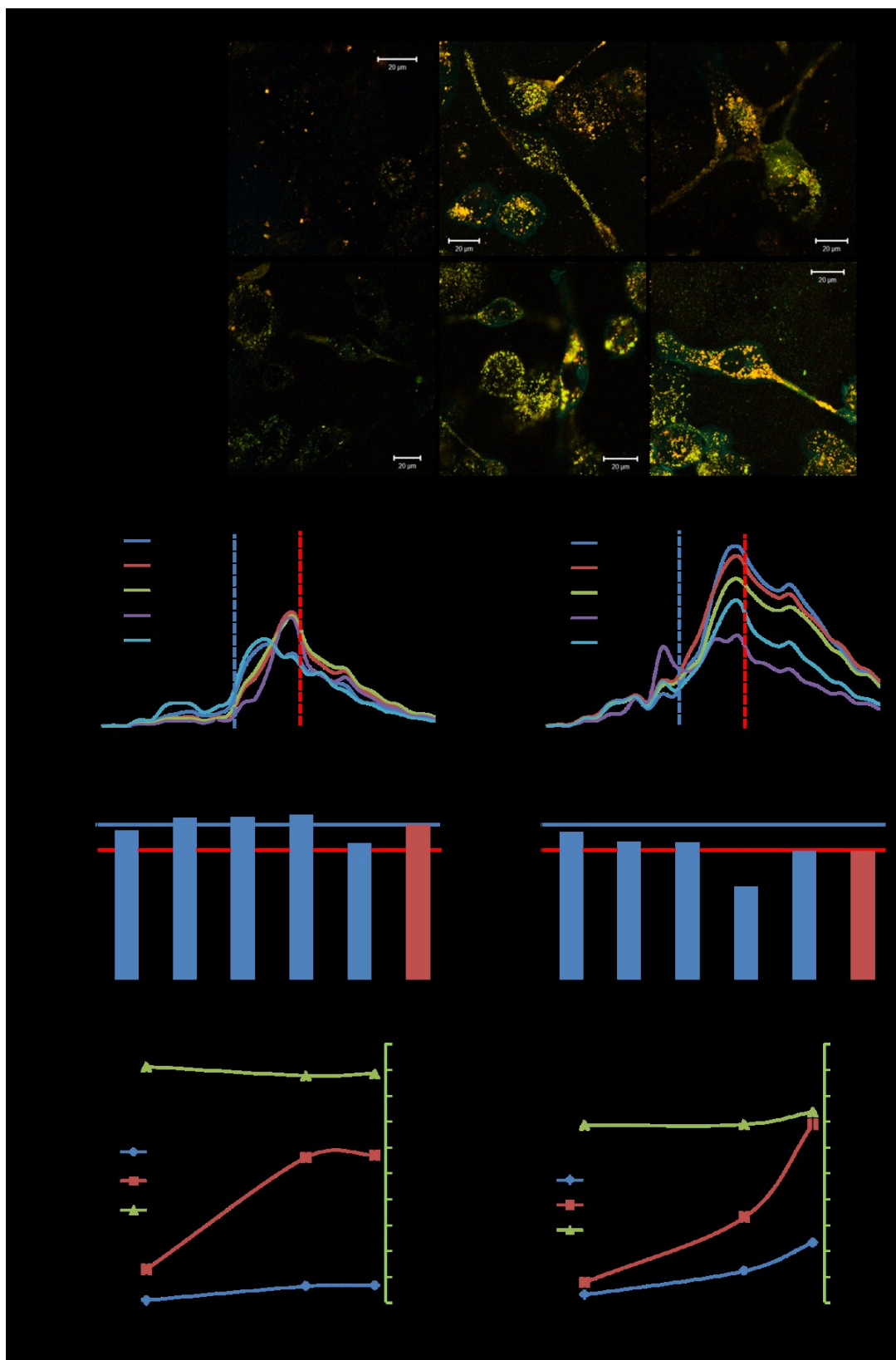


FIGURE 7

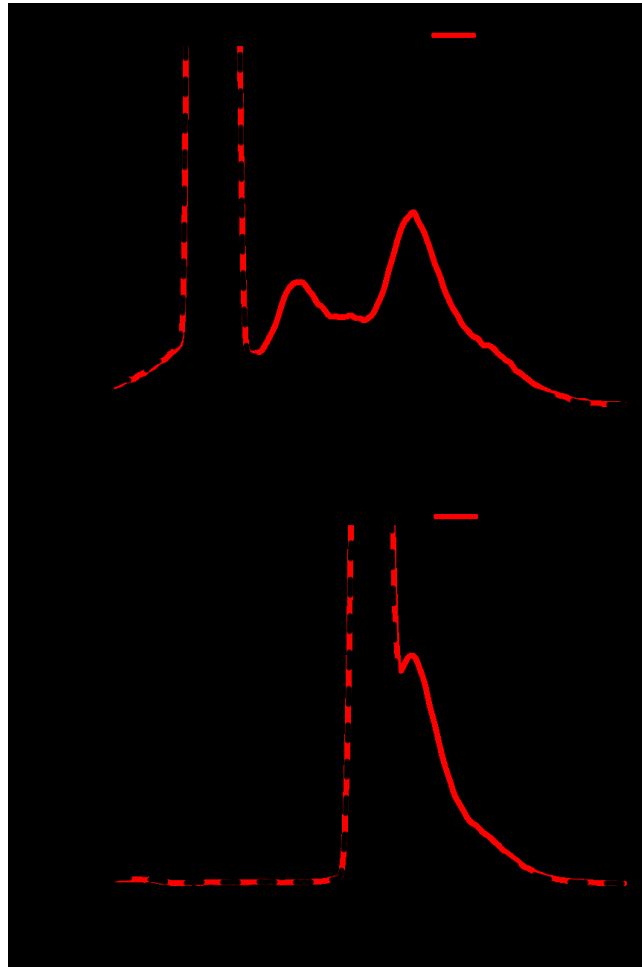


FIGURE 7 CAPTION

Figure 7. Fluorescent emission spectra of DiO₅₀/DiI₅₀ dual-component nanosuspensions and the 1:1 mixture of DiO single-component and DiI single-component nanosuspensions after transport through Caco-2 cell monolayer (incubated at 50 μ M fluorophore concentration); A) Emission spectra of nanosuspensions with an excitation wavelength of 458 nm ($\lambda_{\text{ex}}^{\text{DiO}}$); B) Emission spectra of nanosuspensions with an excitation wavelength of 550 nm ($\lambda_{\text{ex}}^{\text{DiI}}$).

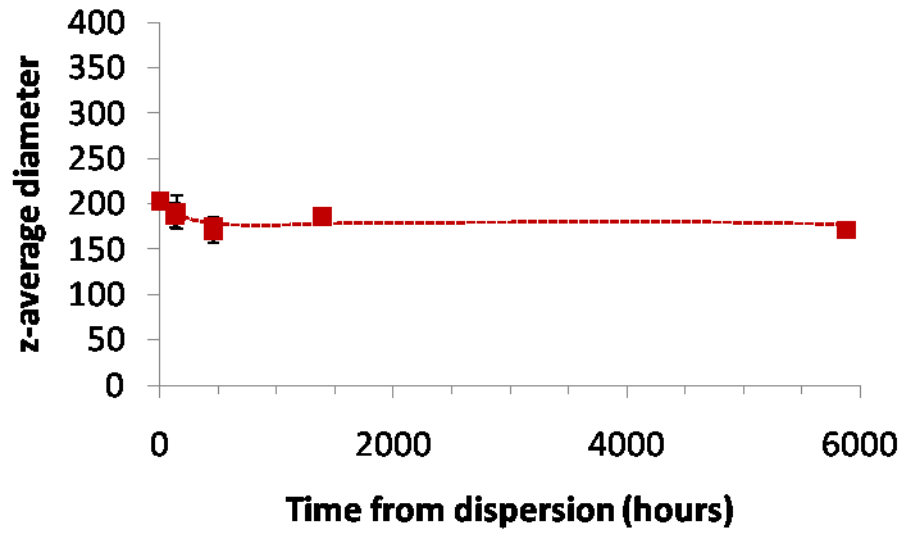


Figure 1S. Stability of the dual-component (DiO₅₀/DiI₅₀) nanosuspension when dispersed in water at 1 mg/ml.

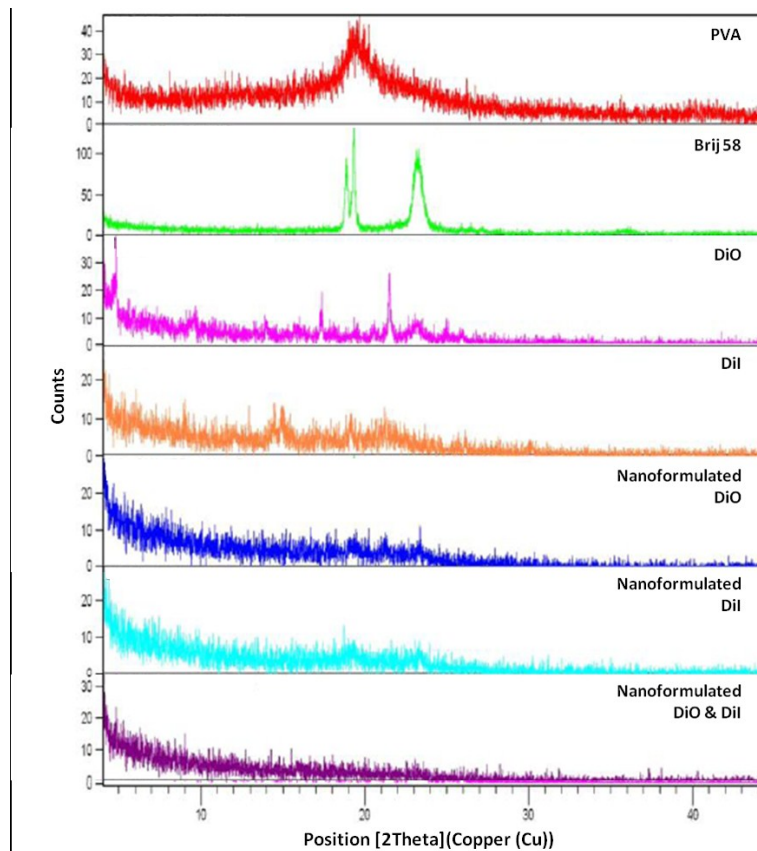


Figure 2S. Powder x-ray diffraction (PXRD) of single and dual-component freeze-dried monoliths (DiO₅₀/DiI₅₀) along with the starting materials used to produce the monoliths.

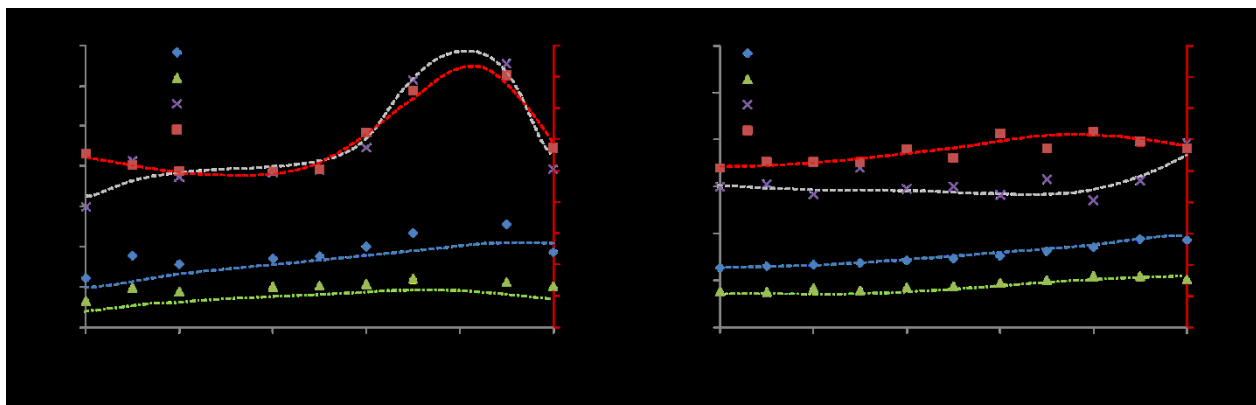


Figure 3S. DLS analysis of the effect of varying the ratio of DiO to DiI in (A) dual-component particles or (B) a mixture of single-component particles of DiO and DiI (nanoparticle concentration of 1 mg/ml).

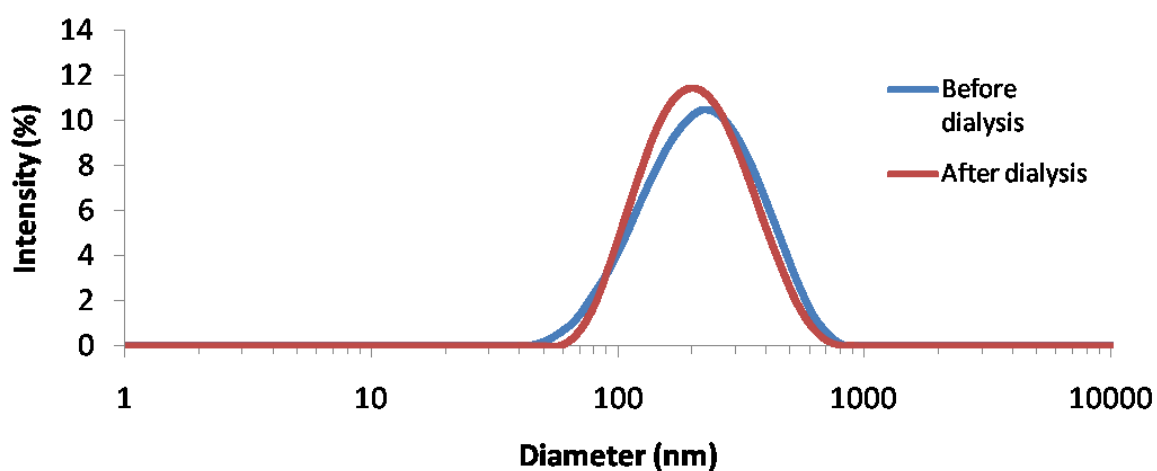


Figure 4S. Effect of 4 days dialysis on the particle size distribution of dual-component (DiO₅₀/DiI₅₀) nanosuspension. Before dialysis the particles had a z-average diameter of 186 nm and afterward the z-average diameter was 181 nm. Samples were analyzed by DLS at a nanoparticle concentration of 0.5 mg/ml.

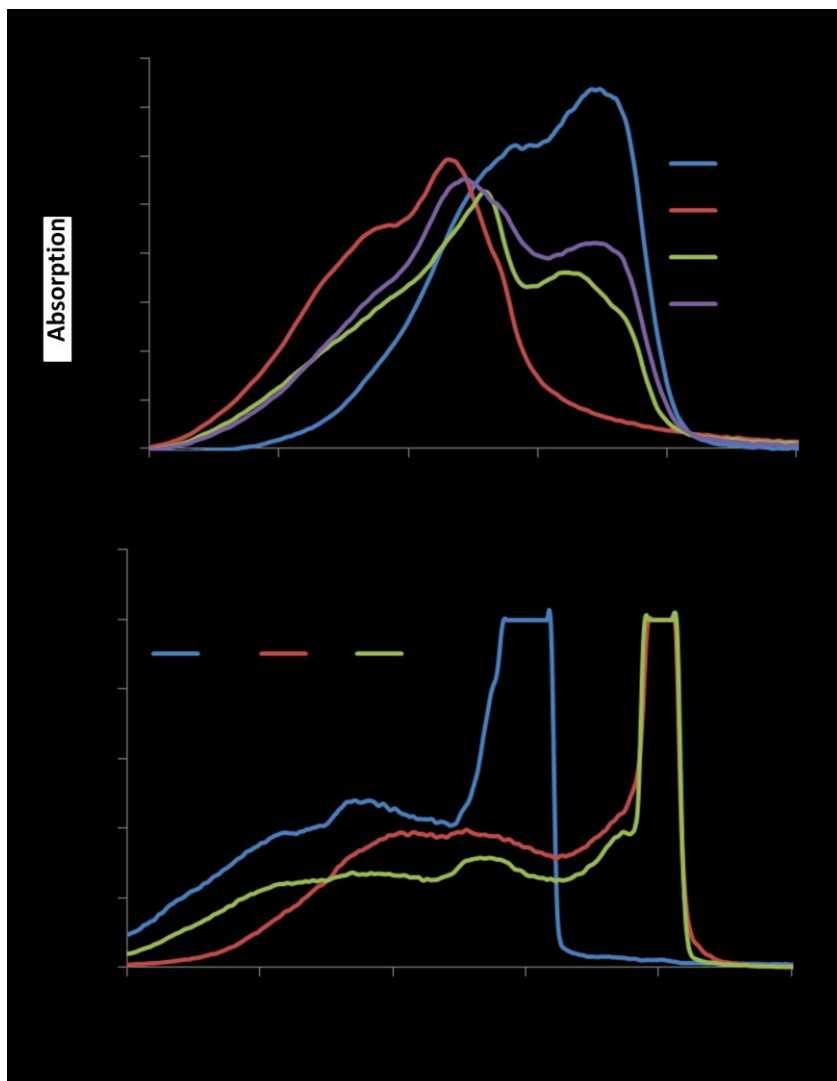


Figure 5S. Absorption (top) and excitation (bottom) spectra for single and dual-component nanosuspensions (DiO₅₀/DiI₅₀). The absorption measurement were obtained at a particle concentration of 0.5 mg/ml (using a Thermo Scientific Nanodrop 2000c in pedestal mode). For the excitation spectra measurements the nanosuspensions were at 0.032 mg/ml and the emission wavelength was set to 550 nm for the DiO nanosuspension and 600 nm for the DiI or dual-component nanosuspensions.

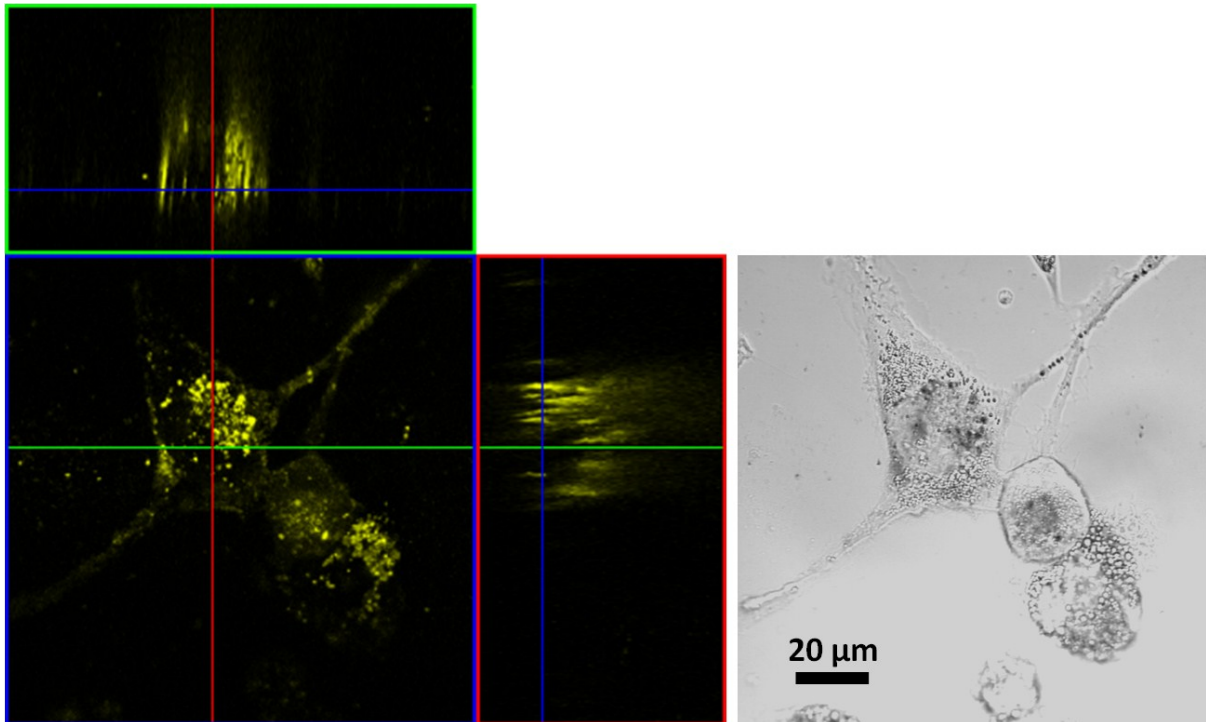


Figure 7S. Orthogonal section of a confocal image of an AHP-1 cell after 24 hours incubation with dual-component nanosuspension in which the focal plane is in the interior of the cells.

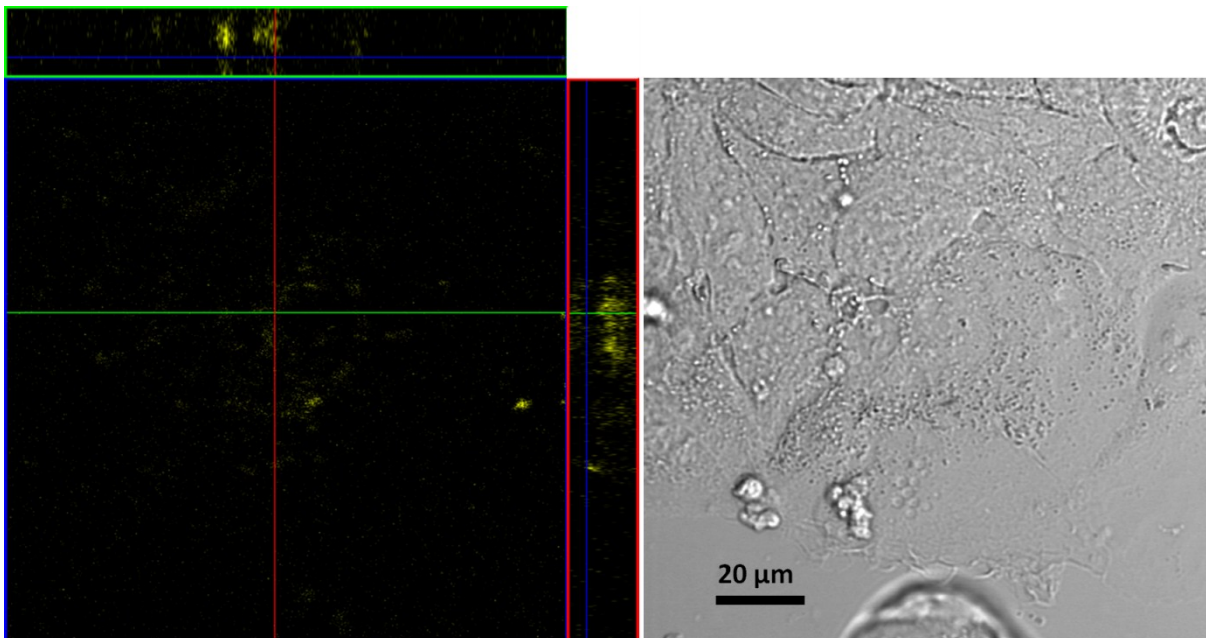


Figure 8S. Orthogonal section of a confocal image of a Caco-2 cell after 19 hours incubation with dual-component nanosuspension in which the focal plane is in the interior of the cells.

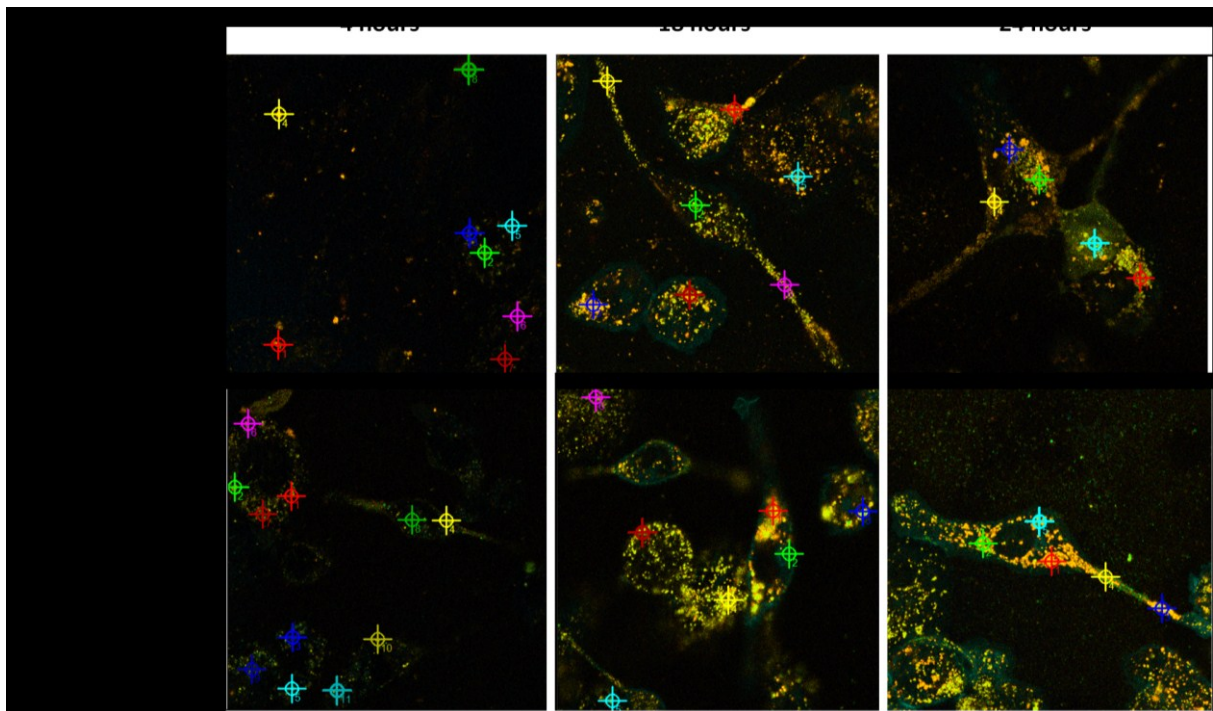


Figure 9S. Confocal microscopy of the A-THP-1 cells incubated with DiO₅₀/DiI₅₀ dual-component nanosuspension or a 1:1 mixture of single-component DiO and single-component DiI nanosuspensions. The ROIs selected for spectral analysis for all time points are shown.

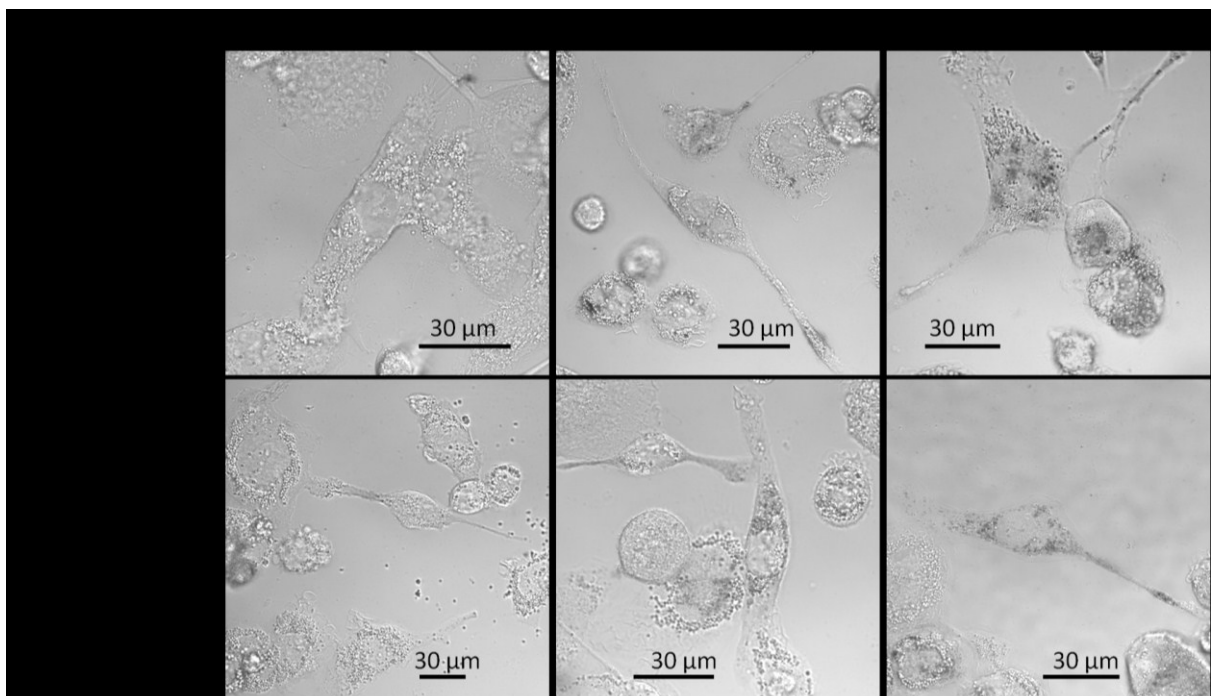


Figure 10S. Brightfield images corresponding to the images obtained by confocal fluorescence microscopy.

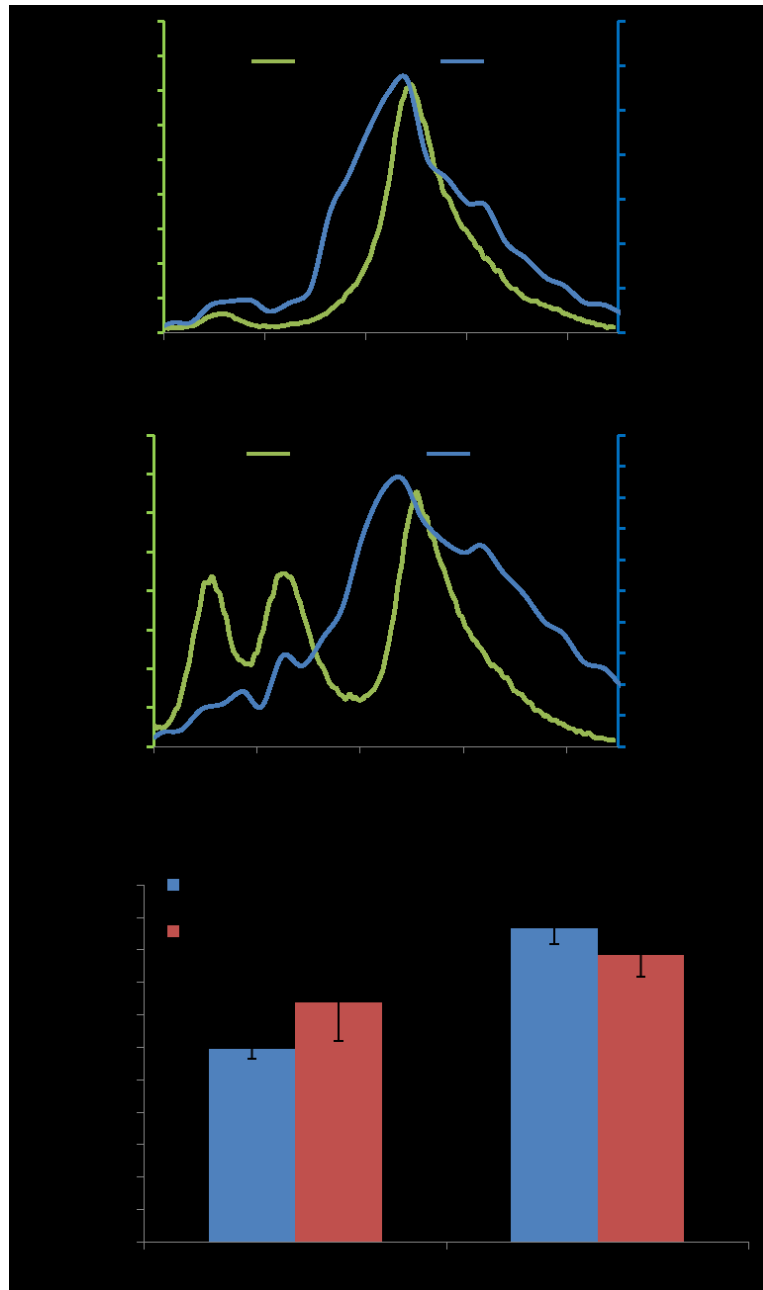


Figure 11S. Comparison of fluorescence emission of dual-component ($\text{DiO}_{50}/\text{DiI}_{50}$) and a mixture of single-component nanoparticles accumulated within the A-THP-1 cells to a free nanosuspension. A: Comparison of the dual-component nanosuspension emission spectra for the nanoparticles accumulated within the A-THP-1 cells to the free nanosuspension. B: Comparison of the mixture of single-component nanosuspensions emission spectra for the nanoparticles accumulated within the A-THP-1 cells to the free nanosuspension. C: The FRET ratios for either the dual-component nanoparticles or mixture of single-component nanoparticles, accumulated within the inside of the cells and as the free nanosuspension.

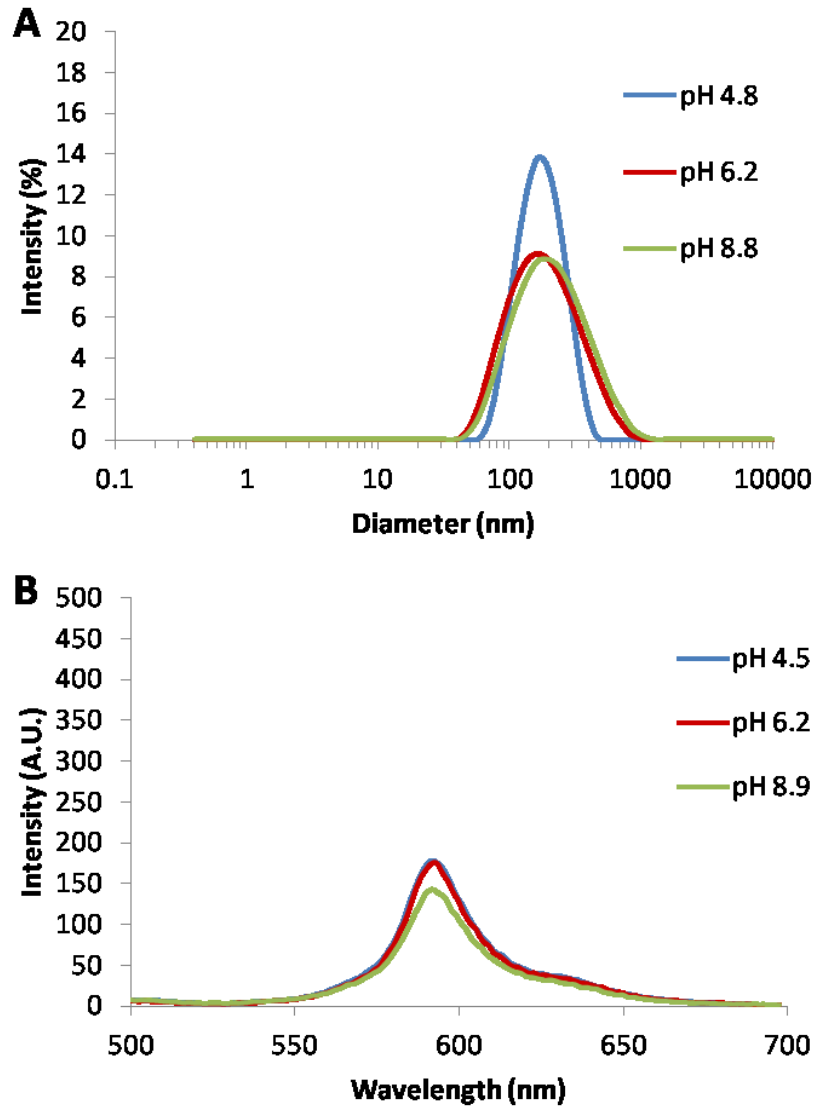


Figure 12S. The effect of pH on the dual-component ($\text{DiO}_{50}/\text{DiI}_{50}$) nanosuspensions. A: DLS analysis of the nanosuspension at three different pHs (particles at 0.1 mg/ml). The z-averages were 151 nm, 159 nm and 159 nm at the pHs of 4.8, 6.2 and 8.8 respectively. B: Fluorescent emission of the dual-component particles at three different pHs using an excitation wavelength of 420 nm (particles at 0.0125 mg/ml). The FRET ratios at the three pH values were 0.97, 0.98 and 0.97 for pH 4.8, 6.2 and 8.8 respectively (FRET ratio was calculated as $\lambda_{595} / (\lambda_{537} + \lambda_{595})$).

